U.S. DEPARTMENT OF COMMERCE
National Technical Information Service

PB-278 342

Mass and Composition of an Urban Aerosol as a Function of Particle Size for Several Visibility Levels

Environmental Sciences Research Lab, Research Triangle Park, N C

10 Jan 77

TECHNICAL REPORT DATA
(Please read Instructions on the reverse before completing)

1. REPORT NO.	2.	3.
EPA-600/J-77-081	JOURNAL ARTICLE	PB 278 342

4. TITLE AND SUBTITLE	5. REPORT DATE
MASS AND COMPOSITION OF AN URBAN AEROSOL AS A FUNCTION OF PARTICLE SIZE FOR SEVERAL VISIBILITY LEVELS	6. PERFORMING ORGANIZATION CODE
7. AUTHOR(S) R.K. Patterson & J. Wagman	8. PERFORMING ORGANIZATION REPORT NO.
9. PERFORMING ORGANIZATION NAME AND ADDRESS Environmental Sciences Research Laboratory - RTP, NC Office of Research and Development U.S. Environmental Protection Agency Research Triangle Park, NC 27711	10. PROGRAM ELEMENT NO. 1AD912
	11. CONTRACT/GRANT NO.
12. SPONSORING AGENCY NAME AND ADDRESS Environmental Sciences Research Laboratory - RTP, NC Office of Research and Development U.S. Environmental Protection Agency Research Triangle Park, NC 27711	13. TYPE OF REPORT AND PERIOD COVERED
	14. SPONSORING AGENCY CODE EPA/600/09

15. SUPPLEMENTARY NOTES
REFERENCE: J. Aerosol Sci., 8: 269-279, 1977

16. ABSTRACT

An atmospheric aerosol sampling analysis experiment at a site near the center of the New York metropolitan area was carried out to delineate relationships existing between degree of visibility and various aerosol characteristics in a polluted atmosphere. Size-fractionated and unfractionated particulate samples were collected at four discrete levels of visibility and analyzed for SO_4^{2-}, NO_3^-, Cl^-, NH_4^+, Pb, Fe, Mg, Zn and total mass.

At all levels of visibility, bimodal or multimodal particle size distributions were observed for total mass and, in some cases, for individual components. Decreased visibility corresponded to increased particle mass concentration especially in the fine particle fraction (ranging in size from about 0.1 to 1.0 μm dia.). Increases in the proportion of particulate sulfate and, to a lesser extent, of nitrate, chloride, ammonium and carbon were also associated with decreased visibility.

17. KEY WORDS AND DOCUMENT ANALYSIS

a. DESCRIPTORS	b. IDENTIFIERS/OPEN ENDED TERMS	c. COSATI Field/Group
*Air pollution *Aerosols *Mass *Chemical composition *Visibility	*Particulate size	13B 07D

REPRODUCED BY
NATIONAL TECHNICAL INFORMATION SERVICE
U. S. DEPARTMENT OF COMMERCE
SPRINGFIELD, VA. 22161

18. DISTRIBUTION STATEMENT	19. SECURITY CLASS (This Report)	21. NO. OF PAGES
RELEASE TO PUBLIC	UNCLASSIFIED	13
	20. SECURITY CLASS (This page) UNCLASSIFIED	22. PRICE A02-A01

EPA-600/J-77-081
JOURNAL ARTICLE

J. Aerosol Sci., 1977, Vol. 8, pp. 269 to 279. Pergamon Press. Printed in Great Britain.

MASS AND COMPOSITION OF AN URBAN AEROSOL AS A FUNCTION OF PARTICLE SIZE FOR SEVERAL VISIBILITY LEVELS

RONALD K. PATTERSON and JACK WAGMAN
U.S. Environmental Protection Agency, Environmental Sciences Research Laboratory, Research Triangle Park, NC 27711, U.S.A.

(*Received* 27 *July* 1976; *and in revised form* 10 *January* 1977)

Abstract—An atmospheric aerosol sampling analysis experiment at a site near the center of the New York metropolitan area was carried out to delineate relationships existing between degree of visibility and various aerosol characteristics in a polluted atmosphere. Size-fractionated and unfractionated particulate samples were collected at four discrete levels of visibility and analyzed for SO_4^{2-}, NO_3^-, Cl^-, NH_4^+, Pb, Fe, Mg, Zn and total mass.

At all levels of visibility, bimodal or multimodal particle size distributions were observed for total mass and, in some cases, for individual components. Decreased visibility corresponded to increased particle mass concentration especially in the fine particle fraction (ranging in size from about 0.1 to 1.0 μm dia.). Increases in the proportion of particulate sulfate and, to a lesser extent, of nitrate, chloride, ammonium and carbon were also associated with decreased visibility.

INTRODUCTION

The integrating nephelometer has been used extensively over the past few years as an atmospheric aerosol monitoring tool (Charlson *et al.*, 1969). The device measures aerosol scattering coefficient (b_{scat}) and is calibrated in reciprocal meters (m^{-1}) using Freon-12 and air. Values of b_{scat} are inversely related to visual range (Koschmieder, 1924) assuming horizontal aerosol homogeneity and negligible light absorption by particles. In this study, size-fractionated and unfractionated urban aerosol samples were collected at several discrete visibility levels and analyzed to determine concentrations and size distributions of total particle mass and selected particle components. The objective was to determine to what extent variations in aerosol mass, composition and particle size distribution are related to variations in visibility in an urban area.

EXPERIMENTAL

A sampling scheme was developed which would yield particle size distribution data for aerosol mass and some chemical constituents with respect to visibility level. The sampling site was located on the grounds of the WWRL radio station's transmitter in Secaucus, New Jersey, approximately 3 miles west of Manhattan, New York. Samples were collected between 29 September and 10 October 1970.

A bank of seven 7-stage Andersen cascade impactors (Andersen, 1966), operated at 1 cfm (28.3 l/min), and one high volume sampler (Hi-Vol, Federal Register, 1971) were separated into three groups, as illustrated in Fig. 1. Group I consisted of a single 7-stage Andersen sampler with 0.001 in. thick stainless steel shimstock on the impactor stages and a 102 mm dia. Gelman Type A glass fiber back-up filter. This group also included the Hi-Vol sampler, operated at a nominal 60 cfm (1.7 m^3/min), used with glass fiber filters. These samplers provided aerosol mass data.

Group II consisted of three 7-stage Andersen samplers, each with the standard stainless steel collection plates and two 90 mm Millipore® back-up filters in series. This group collected particulate matter for analysis of water-soluble components (i.e. sulfate, nitrate, chloride and ammonium ions). Sulfate on the second filter (about 100 μg) was subtracted from that on the front filter to correct for oxidation of adsorbed SO_2 on filter surfaces (Lee and Wagman, 1966).

A.S. 8/4—D

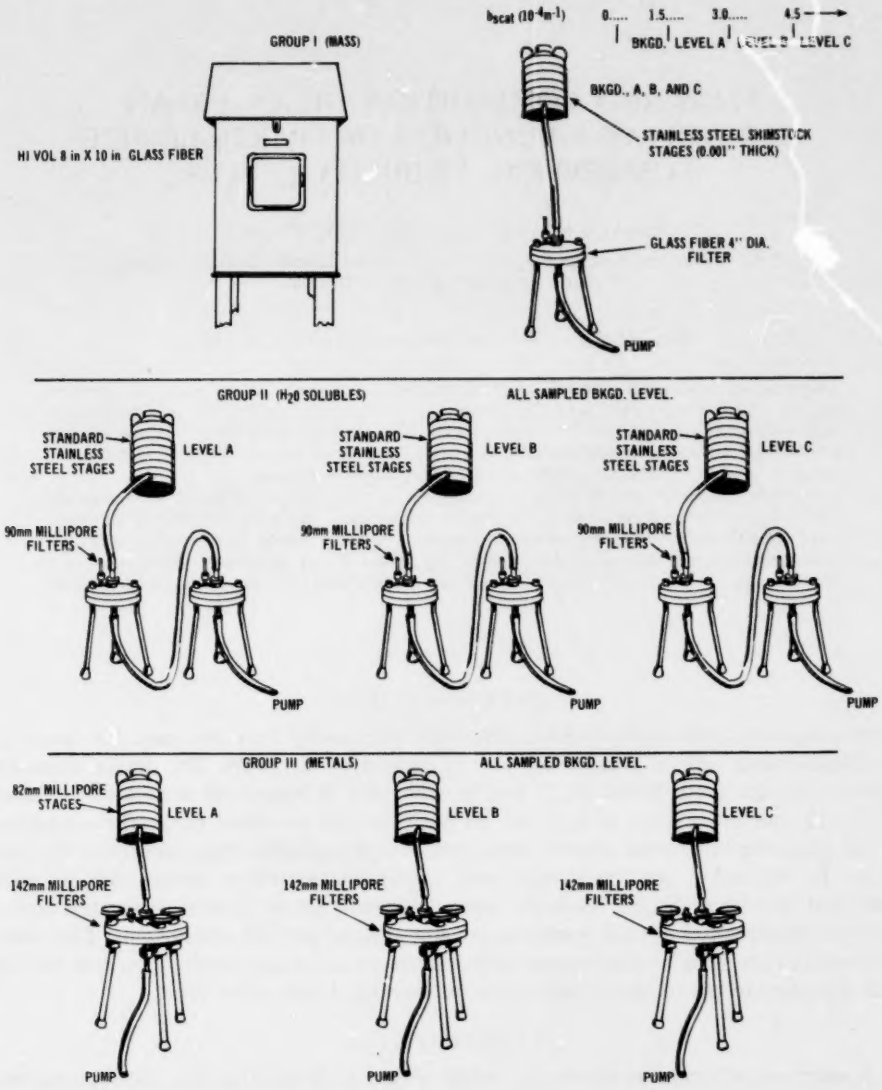

Fig. 1. Equipment used for collecting and size-classifying aerosol samples at various levels of visibility.

Group III consisted of three 7-stage Andersen samplers with 82 mm Millipore® Type AA filters on each impactor stage, and single 142 mm Type AA Millipore® back-up filters. This group collected material for analysis of metals.

Four levels of visibility were chosen. The b_{scat} range of $0–1.5 \times 10^{-4}\,m^{-1}$ was designated as background level, $1.5–3.0 \times 10^{-4}\,m^{-1}$ as level A, $3.0–4.5 \times 10^{-4}\,m^{-1}$ as level B, and $> 4.5 \times 10^{-4}\,m^{-1}$ as level C. An integrating nephelometer (Meteorology Research, Inc., Model 1500) containing a flash lamp with peak response at 440 nm was used to monitor the light scattering coefficient continuously. When the nephelometer indicated that a particular b_{scat} level had been reached, the proper samplers would be started and allowed to run until a different b_{scat} level was attained.

Before any samples were taken at levels A, B and C, background levels samples were collected for 1220 min over a 1-day period. The background run involved sampling with the Hi-Vol and Andersen impactor from Group I (for mass), and all six Andersen impactors in Groups II and III, to collect sufficient sample for chemical analysis.

Since only one Hi-Vol and one Andersen impactor were available for Group I, one Hi-Vol filter and one set of Andersen plates were set aside for each level (A, B and C), and inserted into the samplers whenever visibility levels changed. In Groups II and III, where there were three Andersens available, one in each group was assigned a visibility level (A, B and C) and was simply turned on and off as b_{scat} levels changed. The level A samples were collected for 2283 min over 7 days; level B for 1483 min over 6 days; and level C for 1573 min over a 5-day period. The integrating nephelometer and the Andersen samplers were housed inside a 14-ft trailer. The Hi-Vol was located outside and approximately 4 ft above the ground.

Dzubay *et al.* (1976) have recently claimed, as a result of experiments with 20 cfm impactors, that the use of dry, rather than greased, impaction surfaces in cascade impactors leads to distorted size distribution measurements due to particle bounce. Their data, however, indicate that the distortions they observed were probably due more to reentrainment of particles from overloaded deposits rather than to bounce. The 1 cfm impactors used in this study have stage cutoff aerodynamic diameters based on calibrations (Flesch *et al.*, 1967) for dry impactor plates carried out with monodisperse polystyrene latex and methylene blue spheres. Thus, the particle bounce effect, if present, has to a large extent been factored out empirically in the stage calibrations. Moreover, deposit overload was minimized in this study by periodic shifting of impactor plates relative to their corresponding jet plates. The sharp separations observed for some of the chemical species (see Figs. 4–11) are an indication of the quality of size fractionation achieved with these impactors.

ANALYSIS PROCEDURES

The particulate deposits on Group I Andersen stages and Hi-Vol filters for each visibility level were weighed to determine the mass distribution and total mass at each level. The Hi-Vol filter deposits were also used to determine total carbon, hydrogen and nitrogen using the combustion technique described by Patterson (1973).

The Group II Andersen stage impactor plates were agitated for $\frac{1}{2}$ hr in hot distilled water and the back-up filters were refluxed in distilled water. For the background level samples, extracts from the corresponding stages and back-up filters for the three samplers were pooled in order to increase the concentration of components. The extracts of all Group II samples were analyzed for SO_4^{2-}, NO_3^-, Cl^-, and NH_4^+ by Technicon AutoAnalyzers. Sulfates were analyzed by turbidimetric $BaCl_2$ precipitation, nitrates by colorimetric hydrazine reduction and chlorides by a colorimetric ferric thiocyanate technique using Technicon (1969) Industrial Methods 39–69 W, 32-69 W and 11-68 W, respectively. The NH_4^+ was analyzed using an automated colorimetric Nessler reagent method described by Morgan *et al.* (1966). It should be noted here that the Cl^- analysis used has a bromide interference and therefore yields values more closely related to total halide (Zall *et al.*, 1956).

The particulate deposits on Group III Andersen stages and back-up filters were extracted by placing the filters in Phillips beakers and adding 1 ml of concentrated nitric acid and 1 ml of concentrated hydrochloric acid. The beakers were then covered with watch glasses and the filters taken to incipient dryness at below boiling temperature on a hot plate. After the nitric oxide fumes subsided, 1 ml of concentrated nitric acid was added and the samples taken to incipient dryness continually until all traces of color had disappeared from the extracts. The samples were then cooled slightly, taken to a volume of 25 ml with distilled–demineralized water, replaced on the hot plate, reduced in volume to approximately 10 ml, and filtered where necessary. Each of the extracts was then brought to a volume of 30 ml and stored in polyethylene bottles. For background level samples, the Group III stages were pooled just as in Group II. The Group III extracts were then analyzed for Pb, Fe, Mg and Zn by standard atomic absorption spectrophotometric techniques.

Table 1. Carbon, hydrogen, nitrogen and total particle mass in Hi-Vol samples at various levels of visibility

Visibility level	Visual range (km)	b_{scat} (10^{-4} m^{-1})	Total mass (μg/m^3)	C (μg/m^3)	C (%)	H (μg/m^3)	H (%)	N (μg/m^3)	N (%)
Bkgd	>26	0–1.5	59.1	10.9	18.4	2.1	3.6	1.0	1.7
A	13–26	1.5–3	143	21.1	14.8	3.3	2.3	3.0	2.1
B	8–13	3–4.5	232	37.5	16.2	6.3	2.7	6.7	2.9
C	<8	>4.5	284	46.7	16.4	6.8	2.4	6.3	2.2

RESULTS AND DISCUSSION

Mass and composition

Measurements of total mass, C, H and N, made from samples collected with high volume samplers, are shown in Table 1. Measurements of concentration as a function of a particle size were made for total mass, SO_4^{2-}, NO_3^-, Cl^-, NH_4^+, Pb, Fe, Mg and Zn from samples collected with Andersen cascade impactors. The concentration and percentage of total mass for these components are shown in Table 2. When the concentration for carbon (from Table 1) is included with the other component concentrations in Table 2, from 49 to 67% of the collected material is identified in terms of the analyzed components. The mass collected with the Andersen impactor was substantially (from 25 to 50%) less than that collected with the high volume sampler. This is probably due to the higher upper particle size cutoff of the Hi-Vol and wall losses in the impactor. A large fraction of the particles between 15 and 50 μm aerodynamic diameter that are collected by the Hi-Vol escape collection by the Andersen sampler.

There appear to be only minor differences in composition between levels A, B and C samples. However, several substantial differences are noted between the background level sample and samples at lower visibilities. There was a striking increase in the concentration and percentage of sulfate in the transition from background to lower levels of visibility. Other atmospheric reaction products, i.e. ammonium and nitrate, also increased substantially, while the percentage of iron decreased. Background level Pb had a particle mass median aerodynamic diameter (MMD) of 0.18 μm, or a mean optical

Table 2. Concentrations of selected particulate components at various levels of visibility

Components	Levels of visibility: Background (μg/m^3)	Background (%)	A (μg/m^3)	A (%)	B (μg/m^3)	B (%)	C (μg/m^3)	C (%)
Impactor mass (total)	44.8		78.5		114		212	
SO_4^{2-}	1.7	3.8	12.1	15.4	14.5	12.7	21.3	10.0
NO_3^-	0.8	1.8	2.6	3.3	5.4	4.7	9.7	4.6
Cl^-	0.3	0.7	0.8	1.0	1.9	1.7	1.3	0.6
NH_4^+	1.8	4.0	4.8	6.1	9.6	8.4	11.4	5.4
Pb	5.1	11.4	2.9	3.7	4.2	3.7	*6.8	3.2
Fe	1.9	4.2	1.3	1.7	1.5	1.3	4.1	1.9
Mg	0.2	0.4	0.4	0.5	0.4	0.4	0.9	0.4
Zn	0.7	1.6	0.6	0.8	1.6	1.4	1.7	0.8
C*	10.9	24.3	21.1	26.9	37.5	32.9	46.7	22.0
% identified		52.2		59.4		67.2		48.9
Hi-Vol mass	59.1		143		232		284	
Missing mass†	14.3	24	64.5	45	118	51	72	25

* Derived from values for total carbon in high volume sampler deposits (Table 1) assuming all carbon-containing material collected with the Hi-Vol would also be collected by the impactor and its back-up filter.

† Mass difference between Hi-Vol and impactor collections and percentage of Hi-Vol mass not collected by the impactor.

Table 3. Concentrations of selected particulate components in particles ≤1.5 μm aerodynamic diameter at various levels of visibility

	Levels of visibility							
	Background		A		B		C	
Components	(μg/m³)	(%)	(μg/m³)	(%)	(μg/m³)	(%)	(μg/m³)	(%)
Mass	14.8		39.7		74.8		138	
SO_4^{2-}	1.7	11.5	12.1	30.5	14.3	19.1	20.9	15.1
NO_3^-	0.8	5.4	1.4	3.5	3.5	4.7	7.3	5.3
Cl^-	0.3	2.0	0.5	1.3	1.4	1.9	0.9	0.7
NH_4^+	1.8	12.2	4.7	11.8	9.5	12.7	10.8	7.8
Pb	4.7	31.8	2.7	6.8	3.7	4.9	6.2	4.5
Fe	0.5	3.4	0.3	0.8	0.4	0.5	1.6	1.2
Mg	0.01	0.1	0.1	0.3	0.1	0.1	0.3	0.2
Zn	0.5	3.4	0.5	1.3	1.4	1.9	1.4	1.0
% identified		69.8		56.3		45.8		35.8

diameter of about 0.06 μm, well below the active light scattering region. The unexpectedly high Pb concentration in the background level sample, and the low Pb MMD value suggest that the air contained large quantities of fresh auto exhaust.

Additional information can be obtained by examining the fine particle component separately. Table 3 shows the relative composition of the mass in particles below 1.5 μm dia. (Andersen stages 5, 6, 7 and back-up filter). All of the components measured except for Mg and Fe are present to a larger extent in the fine particle fraction than in the total particle mass. The quantity of ammonium is sufficient to account for all the anions measured—sulfate, nitrate and chloride—as ammonium salts. However, it is likely that acidic species not fully neutralized in the atmosphere would be further neutralized by ammonia in the laboratory air during sample handling and weighing.

Size distribution of total particle mass

Cumulative semi-log plots for particle mass vs aerodynamic size (shown in Fig. 2) were constructed using size cutoff calibrations reported by Flesch *et al.* (1967) for Andersen stages 2–6 (i.e. 5.35, 2.95, 1.53, 0.95 and 0.54 μm dia., respectively) and cutoff values for stages 1 and 7 (i.e. 9.3 and 0.38 μm) calculated from stage dimensional parameters. Interpolated values for total particle MMD obtained from these plots are listed in Table 4.

At all visibility levels, the smooth curves drawn through the plotted points in Fig. 2 indicate size distributions for particle mass that are at least bimodal. This is seen

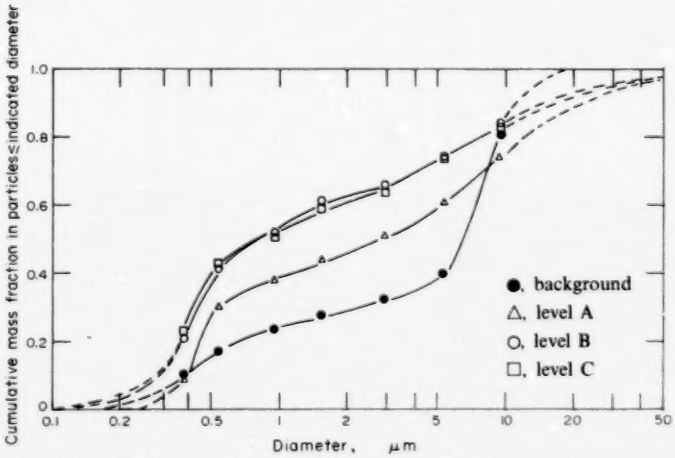

Fig. 2. Cumulative particle mass-size distributions at various visibility levels as determined by size fractionation in a cascade impactor.

Table 4. Total mass and component mass median diameters at various levels of visibility

Components	MMD (μm) Background	A	B	C
SO_4^{2-}	0.60	0.39	0.46	0.40
NO_3^-	0.20	2.6	0.38	0.37
Cl^-	0.17	0.47	0.45	1.1
NH_4^+	0.26	0.34	0.38	0.36
Pb	0.18	0.32	0.38	0.42
Fe	6.6	6.3	5.9	4.5
Mg	>10.0	6.2	6.5	5.5
Zn	1.3	0.76	0.89	0.86
Total mass	6.5	2.8	0.81	0.79

more clearly in Fig. 3, which shows the same data as histogram size plots and as differential mass distribution curves derived from the cumulative curves. Lower and upper size limits of 0.1 and 100 μm, respectively, were selected arbitrarily to construct the end segments of the distributions, and the plots are normalized so that the area under any portion of a histogram or differential curve is proportional to the mass fraction in its corresponding size interval. Thus, the areas included in the end segments are representative of the fractions of mass in particles below 0.4 and above 9 μm dia.

Each of the mass distributions are seen to consist of a fine particle fraction in the size range roughly between 0.1 and 1.0 μm dia., and a coarse fraction consisting of particles exceeding 1–2 μm dia. and constituting the segment beyond the trough in the distribution curve. The fine particle fraction has been referred to elsewhere (Whitby

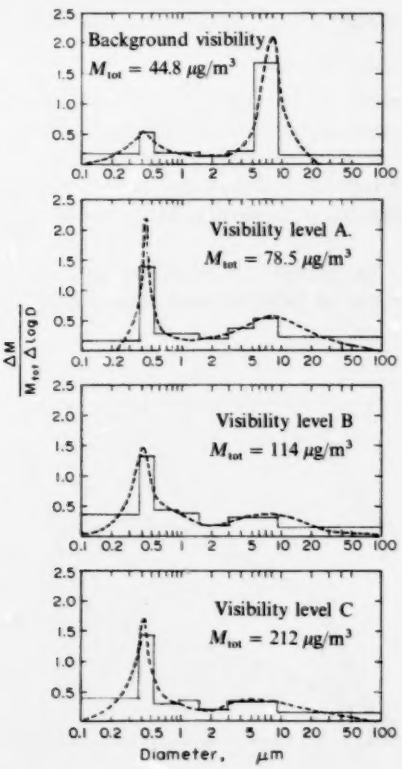
Background visibility
M_{tot} = 44.8 μg/m³
Visibility level A.
M_{tot} = 78.5 μg/m³
Visibility level B
M_{tot} = 114 μg/m³
Visibility level C
M_{tot} = 212 μg/m³
$\frac{\Delta M}{M_{tot} \Delta \log D}$
0.1 0.2 0.5 1 2 5 10 20 50 100
Diameter, μm

Fig. 3. Aerosol mass-size data (from Fig. 2) plotted as histograms and as differential size distributions.

Table 5. Summary of particle size and light scattering parameters at various levels of visibility

Visibility level	Measured b_{scat} range (10^{-4} m^{-1})	Mass concn (μg/m^3)	Fine particle fraction (%)	Fine particle fraction (MMD)	Coarse particle fraction (%)	Coarse particle fraction (MMD)	Calculated b_{scat} (10^{-4} m^{-1})
Bkgd	0–1.5	44.8	30	0.48	70	7.8	0.8
A	1.5–3	78.5	42	0.46	58	8.2	2.7
B	3–4.5	114	63	0.45	37	8.3	4.9
C	>4.5	212	61	0.42	39	8.1	8.9

and Cantrell, 1975) as the "accumulation mode", an allusion to the fact demonstrated earlier by Junge (1964) that these particles, though derived from smaller particles by coagulation and condensation, are themselves relatively stable and long-lived.

The distribution of particle mass between the two size fractions and the median sizes of the fractions at each visibility level are summarized in Table 5. Ensor *et al.* (1972) have calculated distributions of light scattering coefficients with particle size from observed aerosol size distributions by assuming that particles aerodynamically equivalent to unit density spheres are equivalent optically to corresponding unit density spheres of refractive index 1.5. Their calculations show the dominant contribution of the fine particle fraction to total light scattering by aerosols. The application of this procedure to the size distributions shown in Fig. 3, for incident light at 550 nm wavelength, yielded calculated b_{scat} values (listed in Table 5) that correspond reasonably well to the measured b_{scat} ranges. It is evident that the increased proportion of aerosol mass in the fine particle fraction was a major factor, along with higher total particle mass concentration, in reducing visibility from background level to level A to level B. However, the reduction in visibility from level B to level C seems to be entirely the result of higher total aerosol concentration, in view of the nearly identical particle size distributions at these two levels.

Size distribution of individual components

Cumulative size distribution plots were also prepared for the individual components. Interpolated values for component MMDs are listed in Table 4. Sulfate, ammonium and lead had values for MMD of 0.6 μm or less for all visibility levels. The MMD for nitrate was in the 0.2–0.4 μm range except for visibility level A when it was 2.6 μm,

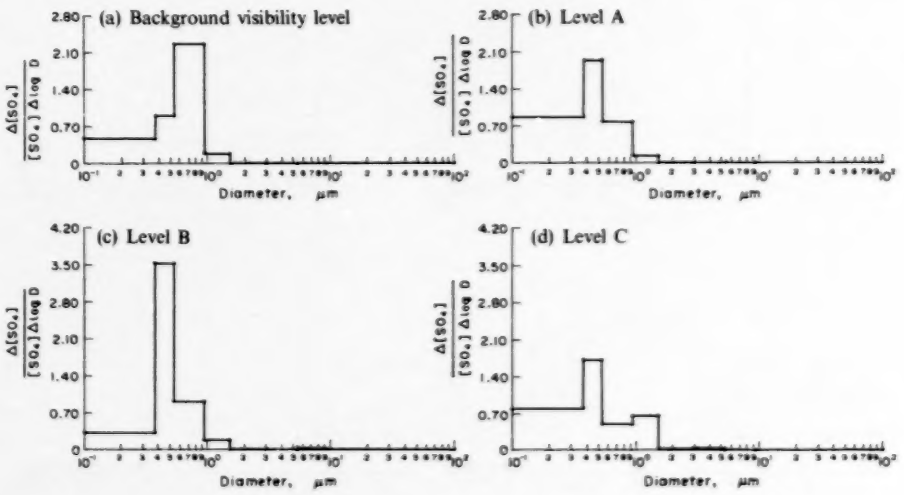

Fig. 4. Particle size histograms for sulfate.

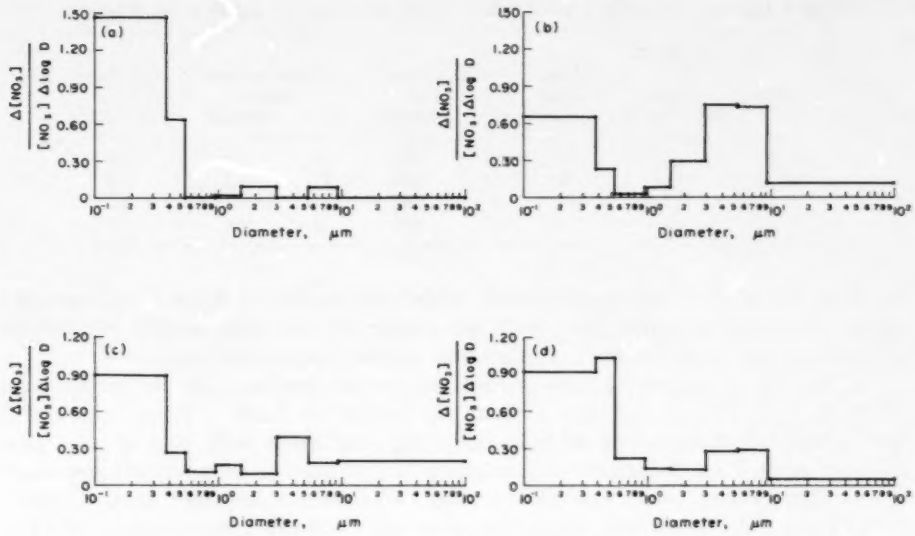

Fig. 5. Particle size histograms for nitrate. (a)–(d), as in Fig. 4.

an observation for which we have no satisfactory explanation at this time. As visibility was reduced, the chloride MMD trended upward from 0.17 to 1.1 μm, while the zinc MMD shifted from 1.3 μm to a lower (0.8–0.9 μm) value. In contrast, the iron and magnesium MMD values were 4.5 μm or higher at all levels of visibility.

Histograms were also prepared for the individual components and are shown in Fig. 4–11. However, attempts to fit differential size distribution curves to these data generally yielded results that were less than satisfactory and were abandoned.

Sulfate and ammonium were observed almost entirely in the fine particle fraction and iron and magnesium in the coarse particle fraction. This suggests single, or groups of similar, sources for these components. Nitrate was present in both the fine and coarse fractions, which suggests two different types of sources or formation mechanisms.

The other components had more complex size patterns. Chloride appeared to have a trimodal distribution; perhaps a sea salt contribution centering at 0.7 to 0.8 μm in

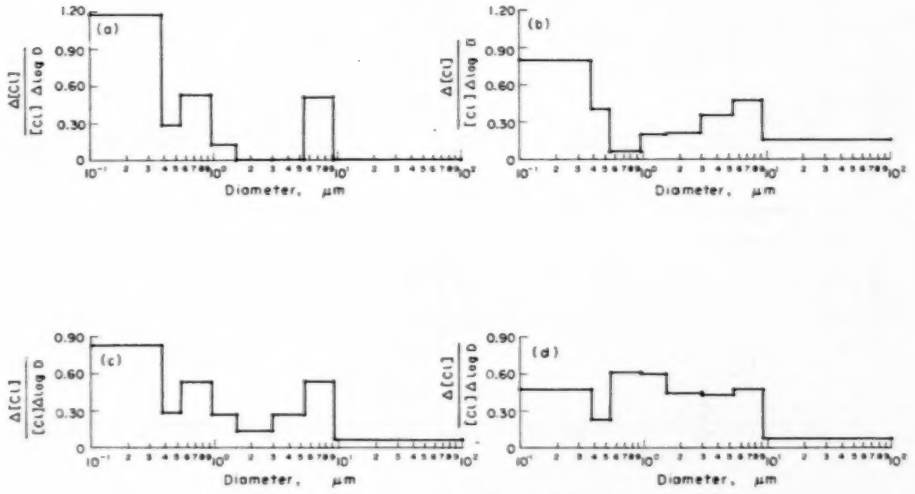

Fig. 6. Particle size histograms for chloride. (a)–(d), as in Fig. 4.

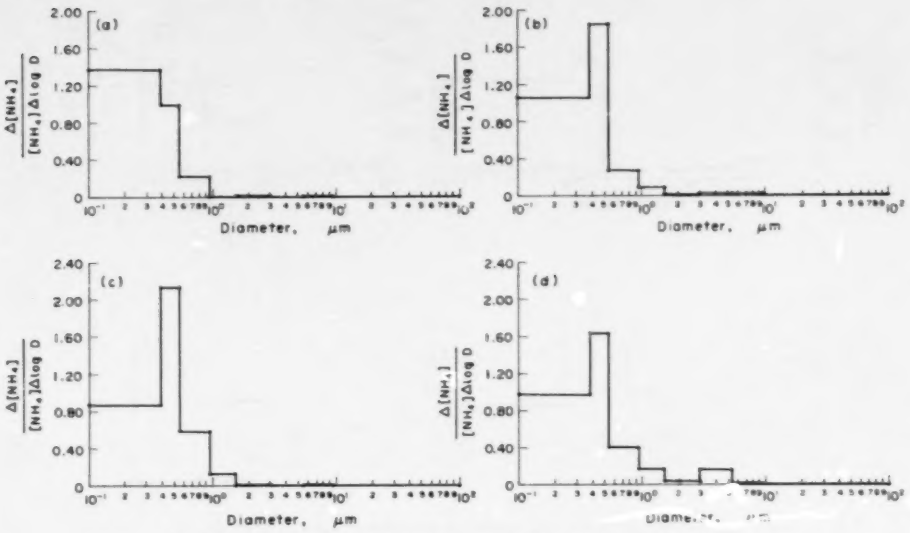

Fig. 7. Particle size histograms for ammonium. (a)–(d), as in Fig. 4.

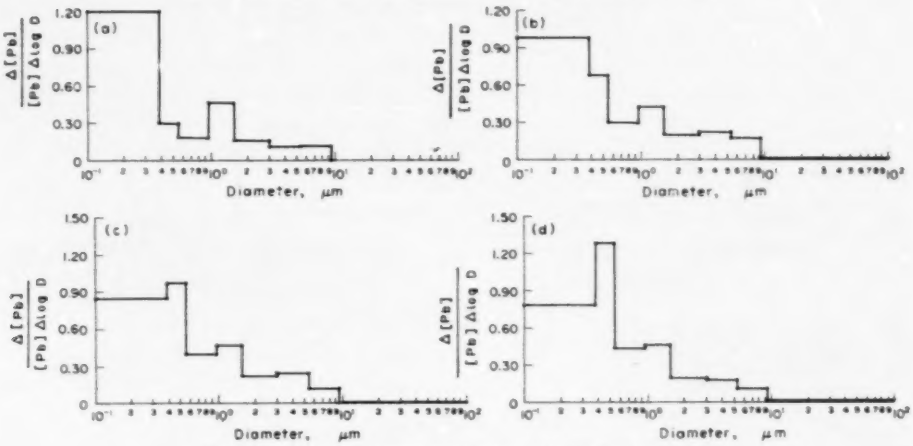

Fig. 8. Particle size histograms for lead. (a)–(d), as in Fig. 4.

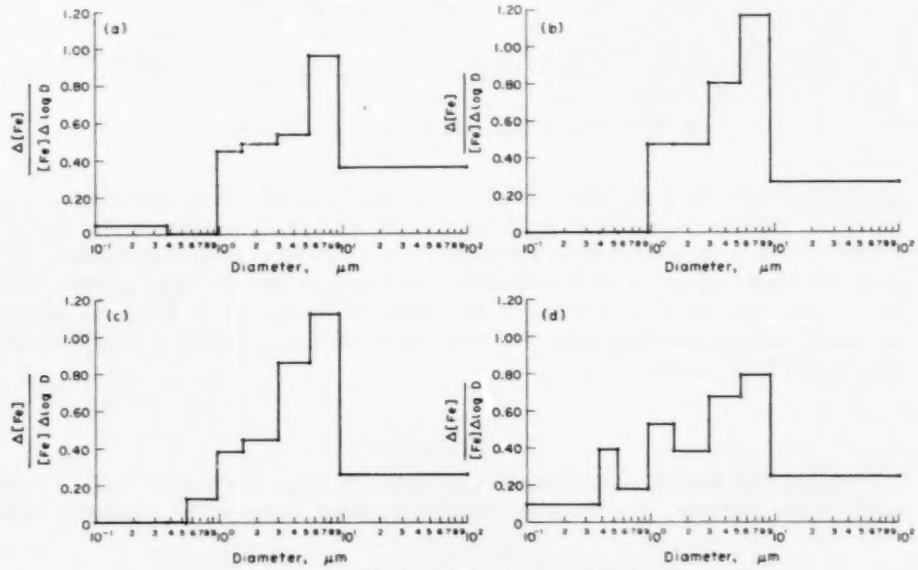

Fig. 9. Particle size histograms for iron. (a)–(d), as in Fig. 4.

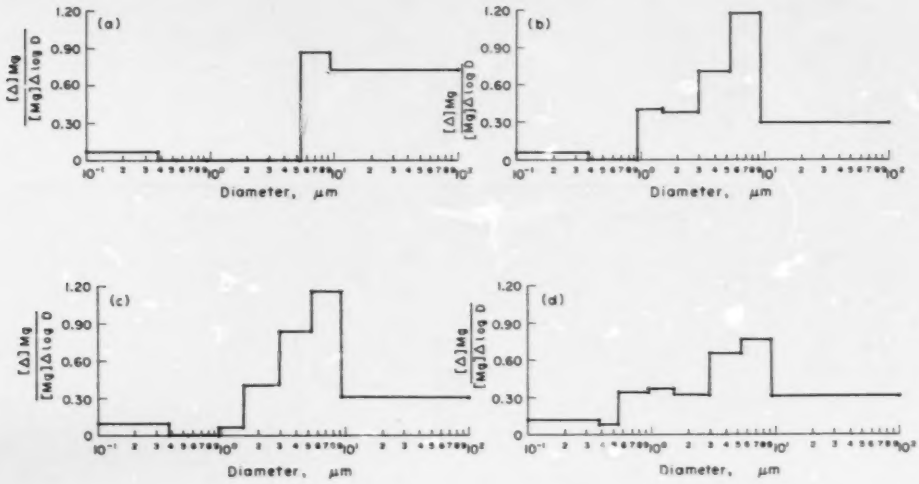

Fig. 10. Particle size histograms for magnesium. (a)–(d), as in Fig. 4.

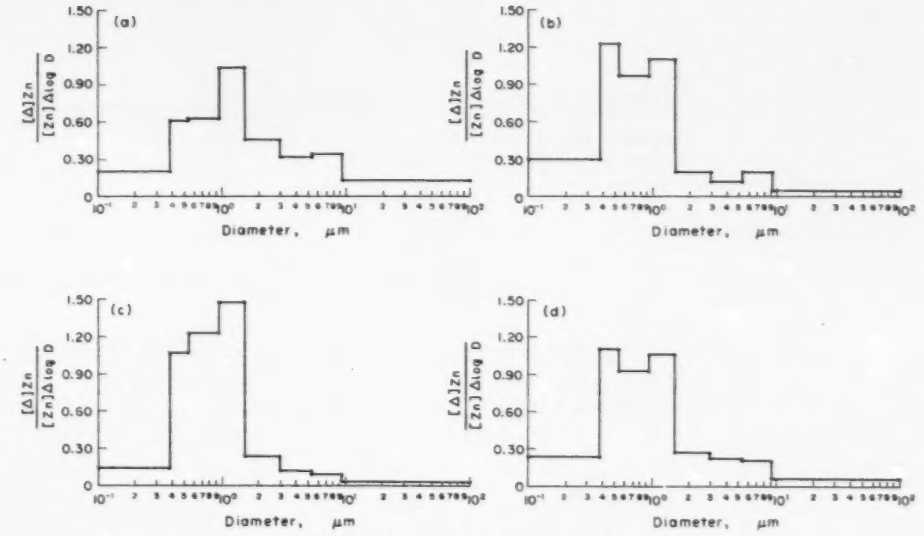

Fig. 11. Particle size histograms for zinc. (a)–(d), as in Fig. 4.

addition to very fine and coarse particle modes resulting from fresh auto exhaust and dredging operations, respectively. Lead, as expected, was found mainly in the fine particle fraction derived from auto exhaust. However, it was also seen in coarser particles derived from industrial sources or from reentrained auto exhaust deposits. Zinc is unusual in that a major portion of it is found in the region of the trough in the gross particle size distribution curves. Zinc appears to have two or more sources with varying contributions at different visibility levels.

CONCLUSIONS

Increased total particle mass concentration, especially in the size fraction below 1.5 μm aerodynamic diameter, was the most prominent change found to be associated with

reduced visibility. However, there were other significant changes. At lower levels of visibility (i.e. levels A, B and C as compared to background), the relative proportion of sulfate and, to a lesser extent, of nitrate, chloride, ammonium and carbon, increased, while lead decreased. The size distribution shifted to place a greater fraction of the total mass in particles below 1 μm aerodynamic diameter. The multimodal nature of the particle size distributions for total mass and, in some cases, for individual components was evident at all visibility levels.

Acknowledgements—This study involved substantial amounts of effort by a number of persons other than the authors. William E. Karches and Lowell E. Hines participated in the sample collection phase of the work, Bettie J. Fahrlender and Lowell E. Hines carried out chemical analyses of samples, and Marie C. Garneau and John H. Overton (Northrop Services, Inc.) assisted in some of the data processing.

REFERENCES

Andersen, A. A. (1966) *Am. ind. Hyg. Ass. J.* **27,** 160.
Charlson, R. J., Ahlquist, N. C., Selvidge, H. and MacGready, P. B., Jr. (1969) *J. APCA* **19,** 937.
Dzubay, T. G., Hines, L. E. and Stevens, R. K. (1976) *Atmos. Envir.* **10,** 229.
Ensor, D. S., Charlson, R. J., Ahlquist, N. C. Whitby, K. T., Husar, R. B. and Liu, B. Y. H. (1972) *J. Colloid Interface Sci.* **39,** 242.
Federal Register (1971), Appendix B, Vol. 36 (84), Part II, April 30, 1971.
Flesch, J. P., Norris, C. H. and Nugent, A. E. (1967) *Am. ind. Hyg. Ass. J.* **28,** 507.
Junge, C. (1964) Final Tech. Rep., Contract No. DA 91-591-EUC-2979, U.S. Department of the Army, DDC document no. AD 445873.
Koschmieder, H. (1924) *Beitr. Phys. Atmos.* **12,** 33, 171.
Lee, R. E., Jr. and Wagman, J. (1966) *Am. ind. Hyg. Ass. J.* **27,** 266.
Morgan, G. B., Tabor, E. C., Golden, C. and Clements, H. (1966) Paper presented at 59th Annual Meeting of the APCA, June 1966.
Patterson, R. K. (1973) *Analyt. Chem.* **45,** 605.
Technicon AutoAnalyzer Methodology (1969) Technicon Corporation, Tarrytown, NY.
Whitby, K. T. and Cantrell, B. K. (1975) *Proc. Int. Conf. Environmental Sensing and Assessment*, Vol. 2, Paper 29–1, Las Vegas, Nevada, September, 1975.
Zall, D. M., Fisher, D. and Garner, M. Q. (1956) *Analyt. Chem.* **28,** 1666.